

Polarization in Heavy-Ion Inelastic Scattering in the Coulomb-Nuclear Interference Region

S. G. Steadman, T. A. Belote, R. Goldstein, and L. Grodzins

Laboratory for Nuclear Science, Massachusetts Institute of Technology, Cambridge, Massachusetts 02139*

and

D. Cline and M. J. A. de Voigt

Nuclear Structure Research Laboratory,† University of Rochester, Rochester, New York 14627

and

F. Videbæk

The Niels Bohr Institute, University of Copenhagen, Copenhagen, Denmark

(Received 10 July 1974)

The polarization in the region of Coulomb-nuclear interference has been determined from the γ -ray correlation following excitation of the 856-keV 2^+ state in ^{56}Fe by 43-MeV ^{16}O ions. Elastic and inelastic scattering cross sections were also measured. Dramatic interference effects are observed in the transition amplitudes which can be reproduced by coupled-channel distorted-wave calculations.

Inelastic scattering data for heavy ions exhibit, in certain cases,¹ a narrow and deep minimum in the inelastic cross section at a scattering angle corresponding to a grazing collision. This dip, attributed to Coulomb-nuclear interference, can be reproduced by distorted-wave calculations using several optical potentials.¹ The analysis of such data yields the heavy-ion-nucleus potential in the surface region which is also important for transfer reactions. To understand better the reaction mechanism and to determine the optical-model parameters for these reactions the elastic cross section for 43-MeV ^{16}O ions scattered by ^{56}Fe has been measured along with the inelastic cross section of the 856-keV, 2^+ excited state. The m -state transition amplitudes, which are more sensitive for the Coulomb-nuclear interference, have also been determined from a complete γ -ray angular-correlation measurement as a function of the particle scattering angle. The latter measurement gives a check of the validity of the Coulomb-nuclear interference explanation of the observed behavior. Coupled-channel effects, in particular the reorientation effect due to the nonzero static electric quadrupole moment of the ^{56}Fe 2^+ state,² have also been investigated and shown to be important.

The elastically and inelastically scattered ions were measured at angles from 15° to 110° by using a 43-MeV ^{16}O beam from the Rochester MP tandem Van de Graaff accelerator. The two most-abundant charge states of ions scattered by a 5–10 $\mu\text{g}/\text{cm}^2$ isotopically enriched ^{56}Fe target (on a 10 $\mu\text{g}/\text{cm}^2$ carbon backing) were detected by two

position-sensitive silicon detectors in the focal plane of the Enge split-pole magnetic spectrometer. The charge-state distribution of scattered ^{16}O ions was measured repeatedly during the experiment. Since the two most-abundant charge states contained at least 75% of the total strength, the uncertainty due to the charge-state distribution was negligible. The elastic cross section, plotted as a ratio to the Rutherford cross section, and the inelastic scattering cross section are shown at the top of Fig. 1. The inelastic scattering data has a minimum at the grazing angle $\varphi_{gr} \approx 80^\circ$ where the elastic cross section displays a maximum.

The de-excitation γ correlation was measured using a 150 $\mu\text{g}/\text{cm}^2$ isotopically enriched ^{56}Fe target on a 20 $\mu\text{g}/\text{cm}^2$ carbon backing. Four silicon surface-barrier particle detectors, masked to subtend 1.8° in the scattering plane, were placed in a hemispherical chamber to detect the scattered ^{16}O ions. Six 3 in. \times 3 in. NaI(Tl) γ -ray detectors were placed at 15 cm from the target and at any angle in the upper hemisphere. Data for any one of the six γ detectors in coincidence with any one of the four particle detectors (24 independent measurements) were simultaneously collected. A time resolution of 1.3 nsec (full width at half-maximum) was sufficient to discriminate against contaminant groups mainly from transfer reactions which had different times of flight. The particle and γ energy, time difference, and counter identification were stored event by event on magnetic tape and subsequently analyzed using the Rochester Nuclear Structure Research Labor-

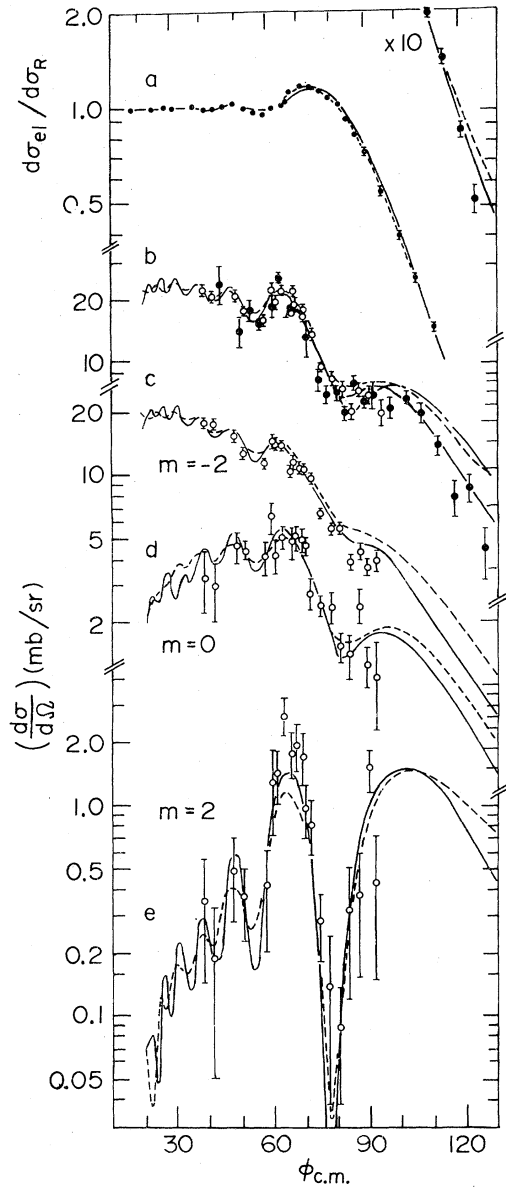


FIG. 1. As a function of the c.m. scattering angle, (a) the ratio of elastic to Rutherford cross sections, (b) the inelastic cross section to the 2^+ state, and (c)–(e) the m -substate populations of the 2^+ state. Dots are data with the magnetic spectrometer; open circles are γ -ray angular-correlation data. The solid lines show the coupled-channel calculation results, the dashed lines show distorted-wave Born-approximation (DWBA) predictions and the dotted line in (b) shows the coupled-channel calculation assuming $Q_{2+} = 0$. The quantization axis is chosen in the direction $\vec{k}_i \times \vec{k}_f$.

atory PDP-6, PDP-8 data-acquisition system.³ Measurements were performed at 28 particle detector angles in the range $\phi_{c.m.} = 38^\circ$ to 131° and many γ angles, giving a total of about 550 data

points, each with statistics of a few hundred counts.

The de-excitation γ -correlation data are sufficient to determine completely the transition amplitudes for any particle scattering angle. The transition amplitudes are most conveniently expressed in a coordinate system in which the x axis is along the beam direction and the z axis is in the $\vec{k}_i \times \vec{k}_f$ direction. In this system the odd- m amplitudes are zero, and the three magnitudes $|T_{+2}|$, $|T_{-2}|$, and $|T_0|$ and two relative phases $\delta_{+2} - \delta_{-2}$ and $\delta_0 - \delta_{-2}$ of the even amplitudes completely determine the transition.⁴ Furthermore, the in-plane γ correlation depends only on the ± 2 transition amplitudes. For a point detector the in-plane angular correlation is given by

$$\omega(\theta_\gamma = 90^\circ, \varphi_\gamma) = A - B \cos[4(\varphi_\gamma - \varphi_0)], \quad (1)$$

where

$$A = (5/16\pi)(|T_{+2}|^2 + |T_{-2}|^2), \quad (2)$$

the anisotropy

$$B/A = 2|T_{+2}||T_{-2}|/(|T_{+2}|^2 + |T_{-2}|^2), \quad (3)$$

and the symmetry angle

$$\varphi_0 = \frac{1}{4}(\delta_{+2} - \delta_{-2}). \quad (4)$$

The $m = 0$ transition amplitude $|T_0|$ and relative phase $\delta_0 - \delta_{-2}$ are determined by the out-of-plane γ -correlation data. At each scattering angle a least-squares fit to the data was made with the five variables $(d\sigma/d\Omega)_{2+}$, A , anisotropy B/A , and the two relative phases. With these parameters, the identification of the $|T_{+2}|$ and $|T_{-2}|$ amplitudes is ambiguous because of their symmetric dependence in Eqs. (2) and (3). However, at forward angles only the $|T_{-2}|$ component is important, allowing one to assign correctly the transition amplitudes at all angles. The calculated γ correlation included corrections for the finite size of the γ detectors, for the decay in flight of the recoiling nuclei by using the expressions of Lesser,⁵ and for the attenuation of the correlation due to hyperfine interactions (deorientation effect) by assuming a pure magnetic interaction and using attenuation coefficients measured by Lesser *et al.*²

The experimentally determined m -state populations $(d\sigma/d\Omega)_m = |T_m|^2$ are shown as a function of c.m. scattering angle in Fig. 1. The relative phases are shown in Fig. 2. A dramatic dip is observed in the $m = +2$ amplitude accompanied by a large shift in the relative phase $\delta_{+2} - \delta_{-2}$ at $\phi_{c.m.} = 78^\circ$ that is near the grazing angle. This is

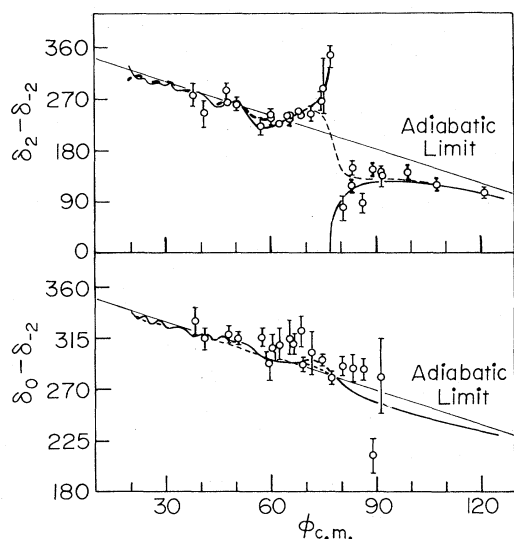


FIG. 2. The relative phases of the transition amplitudes to the 2^+ state as a function of the c.m. scattering angle. The solid lines show the coupled-channel calculation results; the dashed lines show DWBA predictions.

accompanied by a large decrease in the anisotropy and a shift of the symmetry angle of the γ correlation in the scattering plane. At the interference minimum, the recoiling ^{56}Fe are almost completely polarized because here only the $m = -2$ substate contributes to the in-plane γ correlation (Fig. 1) and, therefore, the in-plane correlation is essentially isotropic.

The search program JIB3⁶ was used to find the best Woods-Saxon optical-model parameter set to fit the elastic scattering data. The fitted curve shown in Fig. 1 was obtained for $V = 30.0$ MeV, $W = 7.6$ MeV, $r_0 = 1.30$ fm, $r_i = 1.30$ fm, $a_0 = 0.533$ fm, $a_i = 0.37$ fm, and $r_0^C = 1.25$ fm, values close to those obtained from fits in the Ni isotopes.¹ The optical-model parameters were used in a DWBA calculation of the transition amplitudes using a version of DWUCK⁷ modified to treat the Coulomb excitation properly by including up to 200 partial waves.^{1,8} A collective form factor was used with $B(E2:0^+ \rightarrow 2^+)/e^2 = 974$ fm⁴ and $\beta_2 = 0.23$. This value of β_2 corresponds to an effective isoscaler $B_{1s}(E2:0^+ \rightarrow 2^+)/e^2 = 1200$ fm⁴ with the assumption of a Fermi charge distribution with ^{56}Fe $r_{rms} = 3.825$ fm. The results of this calculation are shown by dashed curves in Figs. 1 and 2. Although these calculations qualitatively exhibit the observed behavior, they are unable to reproduce the $\delta_{+2} - \delta_{-2}$ phase behavior for any reasonable value of $B(E2:0^+ \rightarrow 2^+)$ and β_2 .

A coupled-channel (CC) calculation⁹ was performed with $W = 3.6$ MeV and otherwise using the same parameters, collective form factors, $B(E2)$, and β_2 , and both with and without a rotational value for the excited-state static quadrupole moment ($Q_{2+}/e = -28$ fm², in agreement with experiment.²) These are shown by solid and dotted lines in Fig. 1(b). The complete CC calculation, including the static quadrupole moment, is in excellent agreement with the data. The fit to the elastic scattering data is comparable, but the observed discontinuity for $\delta_{+2} - \delta_{-2}$ is reproduced correctly. The excited-state static quadrupole moment produces a 2° shift in the position of the interference minimum and about a 40% reduction in the back-angle inelastic cross section. One feature of the CC calculation is to reduce the rise of the elastic cross section above the Rutherford prediction by coupling to the 2^+ state, while in the DWBA calculation this is done by an increase of the imaginary potential.

To understand qualitatively the Coulomb-nuclear interference, each transition amplitude is a coherent sum of the Coulomb and nuclear complex amplitudes:

$$T_m = \exp(i\delta_m^C) \{a_m^C - a_m^N \exp[i(\delta_m^N - \delta_m^C)]\}. \quad (5)$$

The oscillating behavior results from the scattering-angle dependence of the phase difference $\delta_m^C - \delta_m^N$, mainly determined by the optical potential. A DWBA calculation has been performed where the Coulomb part and the nuclear part of the form factor were separately set to zero. The nuclear transition amplitude is very small at forward scattering angles, as expected, and behaves similarly for each m substate. However, the Coulomb amplitude varies strongly with the m state, and for the $m = +2$ substate is the smallest, being about the same magnitude as the nuclear amplitude, resulting in the considerably more striking interference effects for this transition amplitude than for the inelastic cross section. The behavior of the phase $\delta_{+2} - \delta_{-2}$ depends on the relative size of the Coulomb and nuclear amplitudes as the Coulomb-nuclear phase passes through zero. That is, the occurrence of the discontinuity in $\delta_{+2} - \delta_{-2}$ as plotted in Fig. 2, depends upon whether the vector difference of the Coulomb and nuclear amplitudes rotates clockwise or counterclockwise through the interference minimum.

We conclude that the dramatic effects seen in the polarization measurements can be entirely understood in terms of Coulomb-nuclear interference. Whereas the conventional DWBA analy-

sis does not account for all the observed features, inclusion of coupled-channel effects proves to be important. In particular, for back-angle scattering the reorientation effect due to a non-zero excited-state quadrupole moment produces an appreciable effect, and in the interference region a correct ratio of the Coulomb to nuclear amplitudes is obtained.

*Supported by U. S. Atomic Energy Commission Contract No. AT(11-1)-3069.

†Supported in part by the National Science Foundation.

¹P. R. Christensen, I. Chernov, E. E. Gross, R. Stokstad, and F. Videbæk, Nucl. Phys. **A207**, 433 (1973).

²P. M. S. Lesser, D. Cline, P. Goode, and R. Horoshko, Nucl. Phys. **A190**, 597 (1972).

³D. Cline, in Proceedings of the Skytop Conference on Computer Systems in Nuclear Physics, Skytop, Pennsylvania, 1969, Columbia University Report No. CONF-690301 (unpublished), p. 106.

⁴R. Rybicki, T. Tamura, and G. R. Satchler, Nucl. Phys. **A146**, 659 (1970).

⁵P. M. S. Lesser, Ph.D. thesis, University of Rochester, 1971 (unpublished).

⁶F. C. Perey, JIB3 (unpublished) (modified to include a larger number of partial waves and smaller integration steps needed in calculation of heavy-ion scattering).

⁷P. D. Kunz, DWUCK, University of Colorado, 1969 (unpublished).

⁸F. Videbæk, unpublished.

⁹W. Brückner, J. G. Merdinger, D. Pelte, U. Smilansky, and K. Traxel, Phys. Rev. Lett. **30**, 57 (1973).

Mass-Yield Distributions in the Reaction of ^{84}Kr Ions with $^{238}\text{U}^\dagger$

J. V. Kratz,* A. E. Norris,† and G. T. Seaborg

Lawrence Berkeley Laboratory and Department of Chemistry, University of California, Berkeley, California 94720

(Received 24 June 1974)

Yields of 156 nuclides were measured radiochemically to delineate the mass distribution in the reaction of 605-MeV ^{84}Kr with thick ^{238}U targets. The yields are consistent with decomposition of the mass distribution into five components: transfer products (700 ± 120 mb), "quasi-Kr" products centered at $A \approx 85$ (470 ± 70 mb) and the products from symmetric fission of their complements (420 ± 60 mb), products from low-energy fission of $Z \approx 92$ nuclides (200 ± 40 mb), products from complete fusion-fission (55 ± 15 mb), and unexplained neutron-deficient yields at $A \approx 195$ (~ 40 mb).

A new phenomenon has been observed in heavy-ion reactions and has been termed "multinucleon transfer,"¹ "quasifission,"² "relaxation phenomena,"³ and "deep inelastic scattering."⁴ These reactions are characterized by energy equilibration without mass equilibration, resulting in (i) two fragments with masses close to the target and projectile masses, (ii) fragment kinetic energies close to the calculated Coulombic repulsion of two normal fission fragments, and (iii) angular distributions distinct from those for complete fusion-fission. For ions with $Z \leq 18$, these new reactions were observed to have modest cross sections¹⁻³ in contrast to the complete fusion process that accounts for an important part of the reaction cross section.⁵ For reactions of ^{84}Kr ions with ^{209}Bi , much of the total interaction cross section goes into the new reaction channel,^{2,4} contrary to expectations, whereas the complete fusion-fission cross sections were

found to be low.^{4,5} The ^{84}Kr results were obtained by measuring fragment-fragment coincidences at correlated angles.

The work reported here is a radiochemical measurement of the mass yield distribution for the reaction of ^{84}Kr with thick targets of ^{238}U . This technique provides yields of radioactive products uniquely characterized with respect to Z and A . The integral nature of these cross sections supplies information that is independent of any assumptions about the reaction mechanism. These data are used below to complement the information about mass distributions obtained in kinematic coincidence measurements, in which masses are deduced indirectly from the laboratory energies of the two fragments by assuming full momentum transfer from the projectile to the combined system. Also, kinematic coincidence measurements lack strict differentiation between inelastically scattered projectiles and